



STRUCTURAL SCIENCE
CRYSTAL ENGINEERING
MATERIALS

Volume 75 (2019)

Supporting information for article:

Structural, energetic and spectroscopic studies of new luminescent complexes based on 2-(2'-hydroxyphenyl)imidazo[1,2-*a*]pyridines and 1,2-phenylenediboronic acid

Sylwia E. Kutniewska, Katarzyna N. Jarzemska, Radosław Kamiński, Anton J. Stasyuk, Daniel T. Gryko and Michał K. Cyrański

Structural, energetic and spectroscopic studies of new luminescent complexes based on 2-(2'-hydroxyphenyl)imidazo[1,2-a]pyridines and 1,2-phenylenediboronic acid

Sylwia E. Kutniewska,^a Katarzyna N. Jarzemska,^{a,*} Radosław Kamiński,^a

Anton J. Stasyuk,^b Daniel T. Gryko,^c Michał K. Cyrański ^a

^a Department of Chemistry, University of Warsaw, Żwirki i Wigury 101, 02-089 Warsaw, Poland

^b Institute of Computational Chemistry and Catalysis, Department of Chemistry, University of Girona, C/ M. Aurèlia Capmany 69, 17003, Girona, Spain

^c Institute of Organic Chemistry, Polish Academy of Sciences, Kasprzaka 44/52, 01-224 Warsaw, Poland

* Corresponding author: Katarzyna N. Jarzemska (katarzyna.jarzemska@gmail.com)

1S. Hansen-Coppens formalism

In the Hansen-Coppens formalism (Hansen & Coppens, 1978), the total atomic electron density (of the k -th atom) is the sum of three components:

$$\varrho_k(\mathbf{r}) = P_{ck}\varrho_{ck}(r) + P_{vk}\kappa_k^3\varrho_{vk}(\kappa_k r) + \sum_{l=0}^{l_{\max}} \sum_{m=-l}^l P_{lmk}\kappa_{lk}'^3 R_{lk}(\kappa_{lk}' r) d_{lmk}(\theta, \varphi)$$

where ϱ_{ck} and ϱ_{vk} are the spherical 1-electron normalized core and valence densities, respectively. The third term contains the sum of the angular functions (d_{lmk}) which model aspherical deformations. The angular functions d_{lmk} consist of real spherical harmonic functions normalised to the electron density. The P_{ck} , P_{vk} and P_{lmk} coefficients stand for populations of the core, valence and deformation density multipoles, respectively. The radial functions (R_{lk}) are defined as:

$$R_{lk}(r) = \frac{\zeta_{lk}^{n_{lk}+3}}{(n_{lk}+2)!} r^{n_{lk}} \exp(-\zeta_{lk} r)$$

where ζ_{lk} and n_{lk} are parameters assigned to each element type separately. κ and κ' are scaling parameters, which control the expansion and contraction of the valence spherical and deformation densities, respectively. For the purpose of this work, each atom was assigned with core and spherical-valence scattering factors derived from Su, Coppens & Macchi wavefunctions (Macchi & Coppens, 2001, Su & Coppens, 1998). In the classical

Hansen-Coppens formalism, P_{vk} , P_{lmk} , κ and κ' constitute the refineable parameters together with the atomic coordinates and thermal motion coefficients.

2S. Structural refinement details

Refinements in the *JANA* program (Petříček *et al.*, 2014) were done according to the transferred aspherical atom model (TAAM). Initial atomic coordinates x , y , and z , and anisotropic atomic displacement parameters (U_{ij} 's; anisotropic ADPs) for each atom were taken from the spherical refinement stage. Initial multipolar and contraction-expansion parameters were transferred from the University at Buffalo Data Bank (UBDB) (Dominiak *et al.*, 2007, Jarzemska & Dominiak, 2012) using the *LSDB* program (Jarzemska & Dominiak, 2012, Volkov *et al.*, 2004), which also assigns optimal local coordinate systems to each atom, scales fragment charges, and standardizes X–H bond lengths (X = non-hydrogen atom) to average neutron distances (Allen *et al.*, 1987) (which were also recently summarised and updated by Allen & Bruno (Allen & Bruno, 2010)). For the purpose of current study, due to the lack of some atoms in the UBDB databank we either transferred the parameters from the atoms with the most similar environments already present in the database, or modelled extra atoms manually according to the original procedure (Jarzemska & Dominiak, 2012). In the case of structures containing more than one independent fragment in ASU, the fragment charges were scaled separately, and all moieties were kept neutral. The multipole expansion was truncated at the hexadecapole ($l_{\max} = 4$) and quadrupole ($l_{\max} = 2$) levels for all non-hydrogen and hydrogen atoms, respectively. In all cases the statistical weights (*i.e.*, $w_i = 1/\sigma_i^2$ for i -th reflection) were applied, the atomic coordinates, ADPs and scale factor were refined, whereas all multipolar parameters were kept fixed. The *JANA* program allows for the application of specific constraints and restraints during the refinement. Consequently, in all the refinements carried out, the hydrogen atom U_{iso} parameters (*i.e.* isotropic thermal parameter) were constrained to the value of $y \cdot U_{\text{eq}}^{\text{X}}$ ($y = 1.2$ and 1.5 for X = C and X = O or N, respectively). The X–H distances were restrained to the literature values with $\sigma = 0.001$ (where an appropriate restraint weight is obviously equal to $1/\sigma^2$). In case of disordered structures some extra restraints and constraints were also used. Such a procedure was found to reproduce very well the neutron-diffraction-quality geometries (Jarzemska *et al.*, 2012). For details characterising all refinements see Table 1S.

Table 1S. Selected X-ray data collection, processing and refinement parameters for all presented crystal structures.#

<i>Structure</i>	odba-a	odba-b	odba-d	b	c
Moiety formula	C ₁₉ H ₁₄ B ₂ N ₂ O ₃ + C ₃ H ₆ O	2 C ₂₀ H ₁₆ B ₂ N ₂ O ₄ + C ₃ H ₆ O	C ₁₉ H ₁₃ B ₂ BrN ₂ O ₃	C ₁₄ H ₁₂ N ₂ O ₂	C ₁₃ H ₉ BrN ₂ O
Moiety formula mass, <i>M_r</i> / a.u.	398.0	798.0	418.9	240.3	289.1
Crystal system	monoclinic	monoclinic	triclinic	orthorhombic	monoclinic
Space group	<i>P</i> 2 ₁ (no. 4)	<i>C</i> 2/ <i>c</i> (no. 15)	<i>P</i> $\bar{1}$ (no. 2)	<i>Pbca</i> (no. 61)	<i>P</i> 2 ₁ / <i>c</i> (no. 14)
<i>a</i> / Å	10.7147(11)	21.8035(16)	8.9492(7)	14.5448(2)	12.8423(7)
<i>b</i> / Å	34.282(3)	10.4647(8)	14.5926(12)	6.5214(4)	7.0971(4)
<i>c</i> / Å	10.9168(11)	19.3032(14)	15.0762(12)	23.8246(6)	12.6239(7)
α / °	90	90	66.778(3)	90	90
β / °	93.176(2)	111.794(3)	82.477(3)	90	107.1883(16)
δ / °	90	90	86.204(3)	90	90
<i>V</i> / Å ³	4003.8(7)	4089.6(5)	1793.5(3)	2259.82(15)	1099.19(11)
<i>Z</i>	8	4	2	8	4
<i>T</i> / K	100	100	100	100	100
<i>F</i> ₀₀₀	1664	1664	840	1008	576
<i>d</i> _{calc} / g·cm ⁻³	1.321	1.296	1.551	1.412	1.747
θ range	2.21° – 29.81°	4.37° – 77.31°	2.96° – 32.73°	3.71° – 77.37°	3.29° – 30.55°
Absorption coefficient, μ / mm ⁻¹	0.089 (Mo K α)	0.732 (Cu K α)	2.314 (Mo K α)	0.786 (Cu K α)	3.722 (Mo K α)
Crystal colour & shape	colourless of unspecified shape	colourless plate	colourless block	colourless of unspecified shape	colourless plate
Crystal size / mm ³	0.29 × 0.13 × 0.06	0.29 × 0.12 × 0.06	0.28 × 0.17 × 0.09	0.20 × 0.14 × 0.11	0.22 × 0.19 × 0.12
No. of reflections collected / unique	99881 / 21060	17247 / 4107	72753 / 12047	18355 / 2331	29038 / 3358

R_{int}	13.54%	5.22%	5.37%	4.20%	4.41%
No. of reflections with $I > 3\sigma(I)$	9603	3264	7212	1831	2530
No. of parameters / restraints	1093 / 4	333 / 13	566 / 26	199 / 12	181 / 9
$R[F] (I > 3\sigma(I))$	5.48%	6.00%	4.80%	3.28%	2.51%
$wR[F^2] (I > 3\sigma(I))$	7.78%	14.92%	9.58%	7.07%	4.51%
$R[F]$ (all data)	17.96%	7.32%	10.69%	4.79%	4.57%
$wR[F^2]$ (all data)	10.16%	15.41%	10.19%	7.51%	5.00%
S (all data)	1.19	2.59	1.97	1.70	1.21
$S (I > 3\sigma(I))$	1.39	2.85	2.43	1.83	1.27
$\rho_{\text{res}}^{\text{min/max}} / \text{e} \cdot \text{\AA}^{-3}$	-0.71 / +0.76	-0.43 / +0.33	-0.79 / +3.73	-0.32 / +0.25	-0.45 / +0.56
CCDC code	1846572	1846573	1846574	1846570	1846571

All raw data are available under the following DOI: 10.18150/repod.5973048.

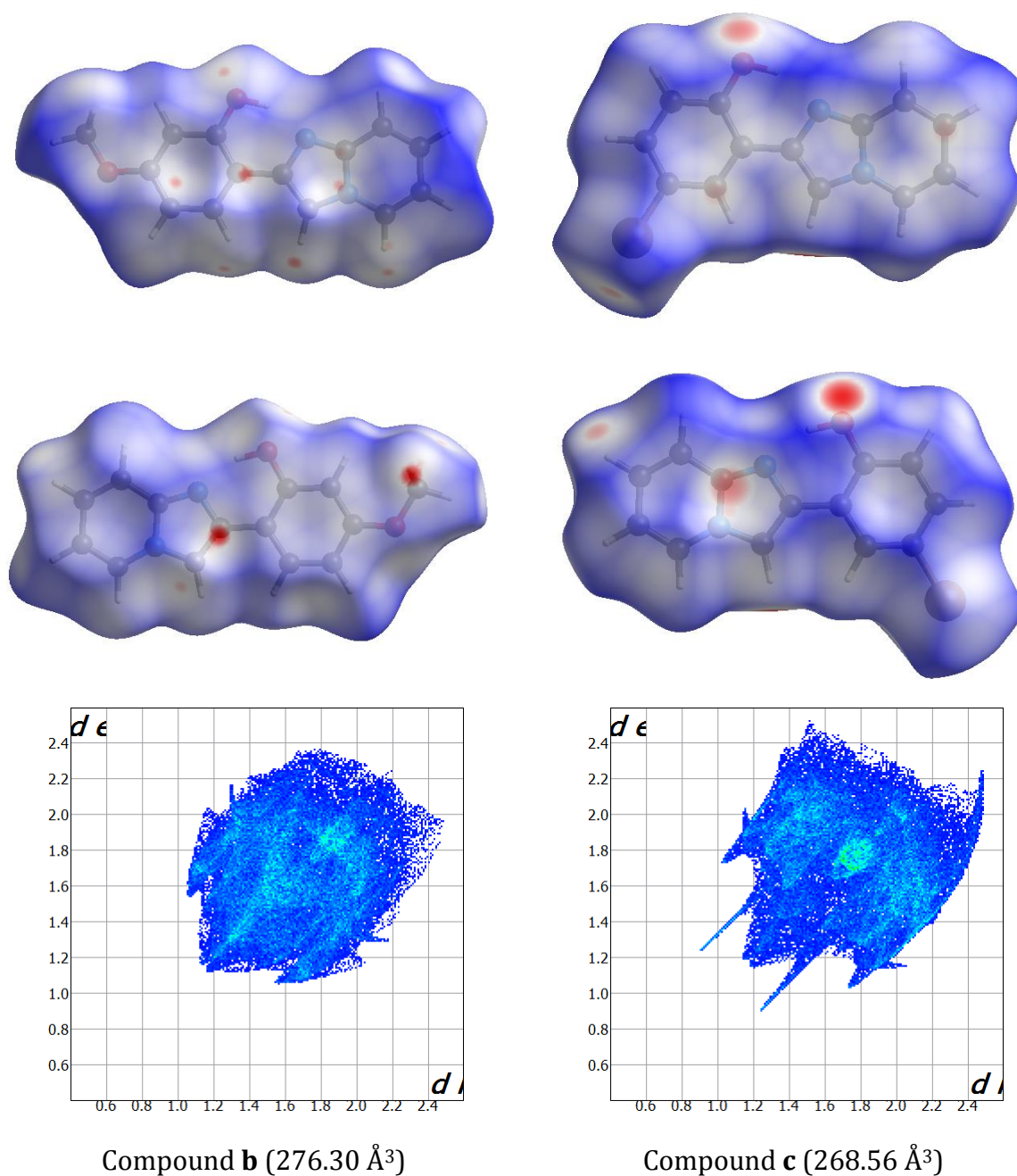


Figure 1S. Hirshfeld surfaces (two orientations, d_{norm} property mapped) and the respective fingerprint plots for compounds **b** (left) and **c** (right). Symbols used: d_e – distance from the surface to the nearest nucleus external to the surface (vertical axes), d_i – distance from the surface to the nearest nucleus internal to the surface (horizontal axes), $d_{\text{norm}} = (d_i - r_i^{\text{vdW}})/r_i^{\text{vdW}} + (d_e - r_e^{\text{vdW}})/r_e^{\text{vdW}}$ – van der Waals (vdW) radii normalised contact distance (red colour – $d_{\text{norm}} < 0$ – distance shorter than vdW contact; blue – $d_{\text{norm}} > 0$ – distance longer than vdW contact). Colours and symbols are retained for all figures.

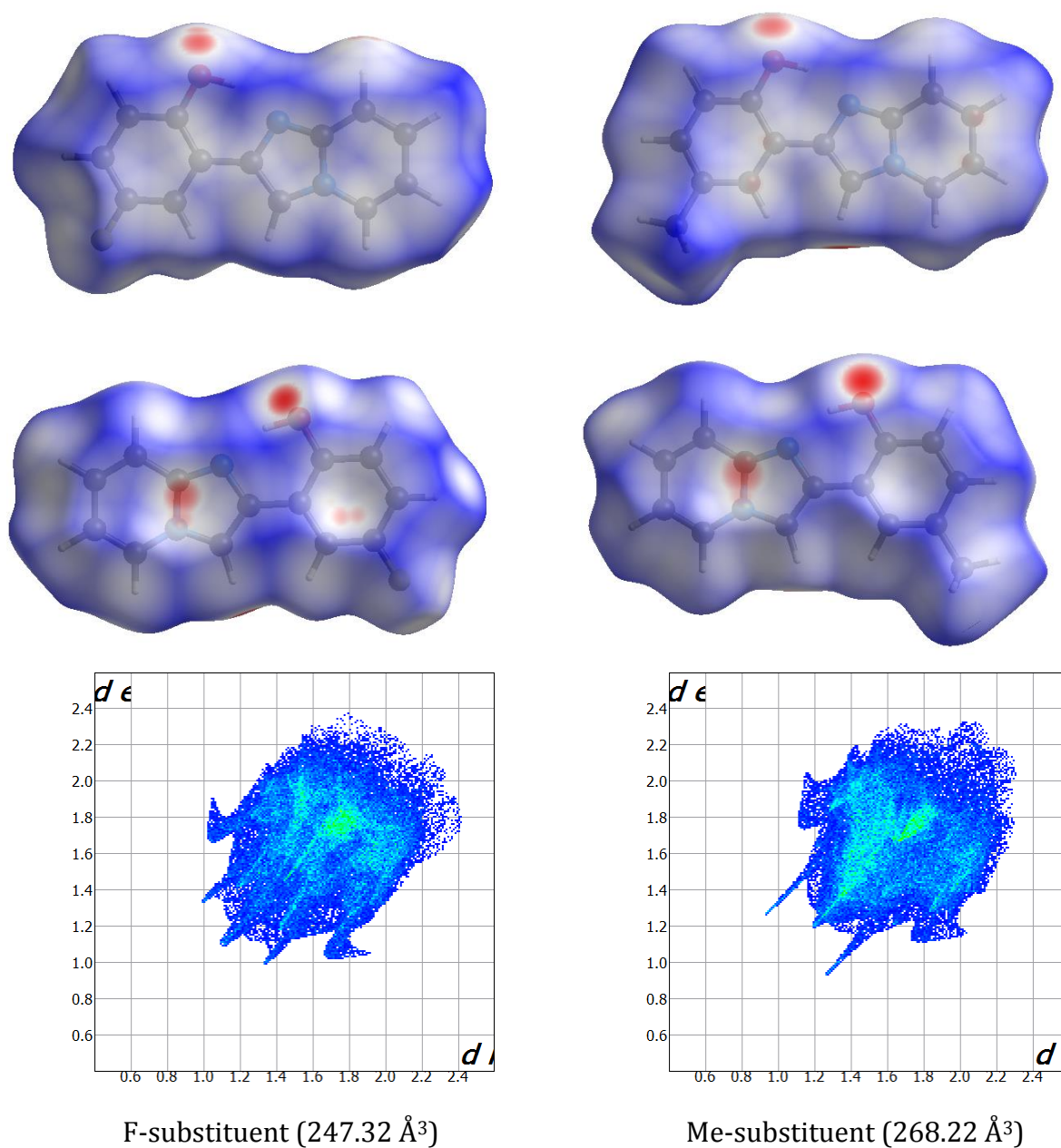


Figure 2S. Hirshfeld surfaces (two orientations, d_{norm} property mapped) and the respective fingerprint plots for literature-retrieved F- (left, CCDC code: 926056) and Me-substituted (right, CCDC code: 926055) compounds.

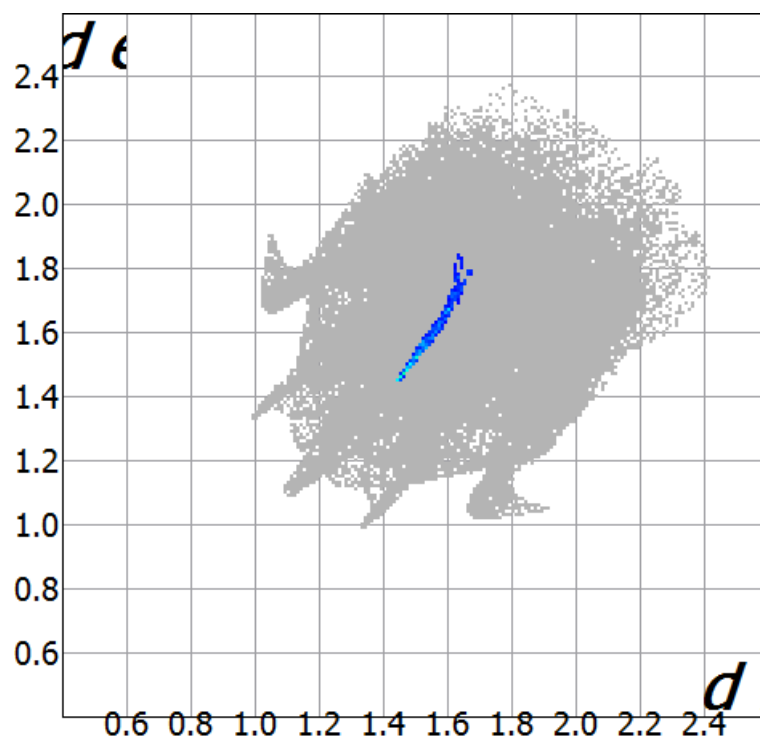


Figure 3S. Fingerprint plot for F-substituted compound (CCDC code: 926056) showing F...F interactions contributing to only 0.8% to the total Hirshfeld surface area.

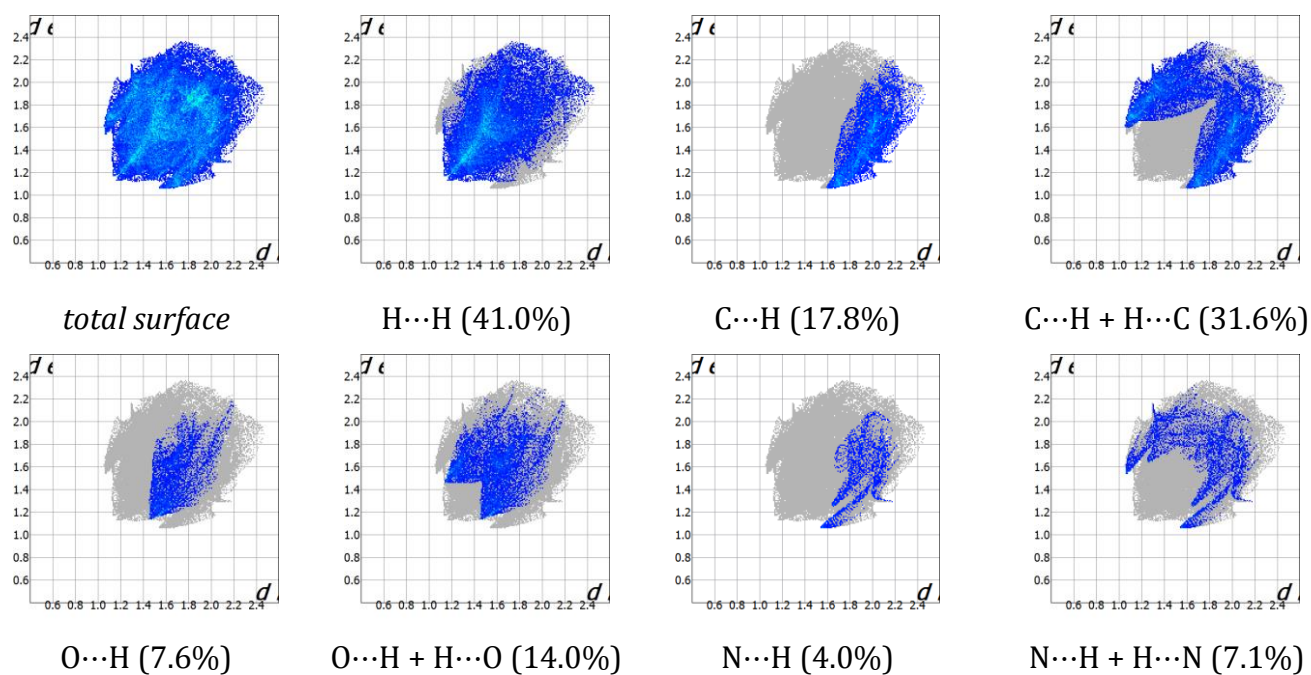


Figure 4S. Hirshfeld surface fingerprint plots for compound **b** showing various interactions contributions to the total surface (in X...Y the X atom is always inside and Y outside the surface).

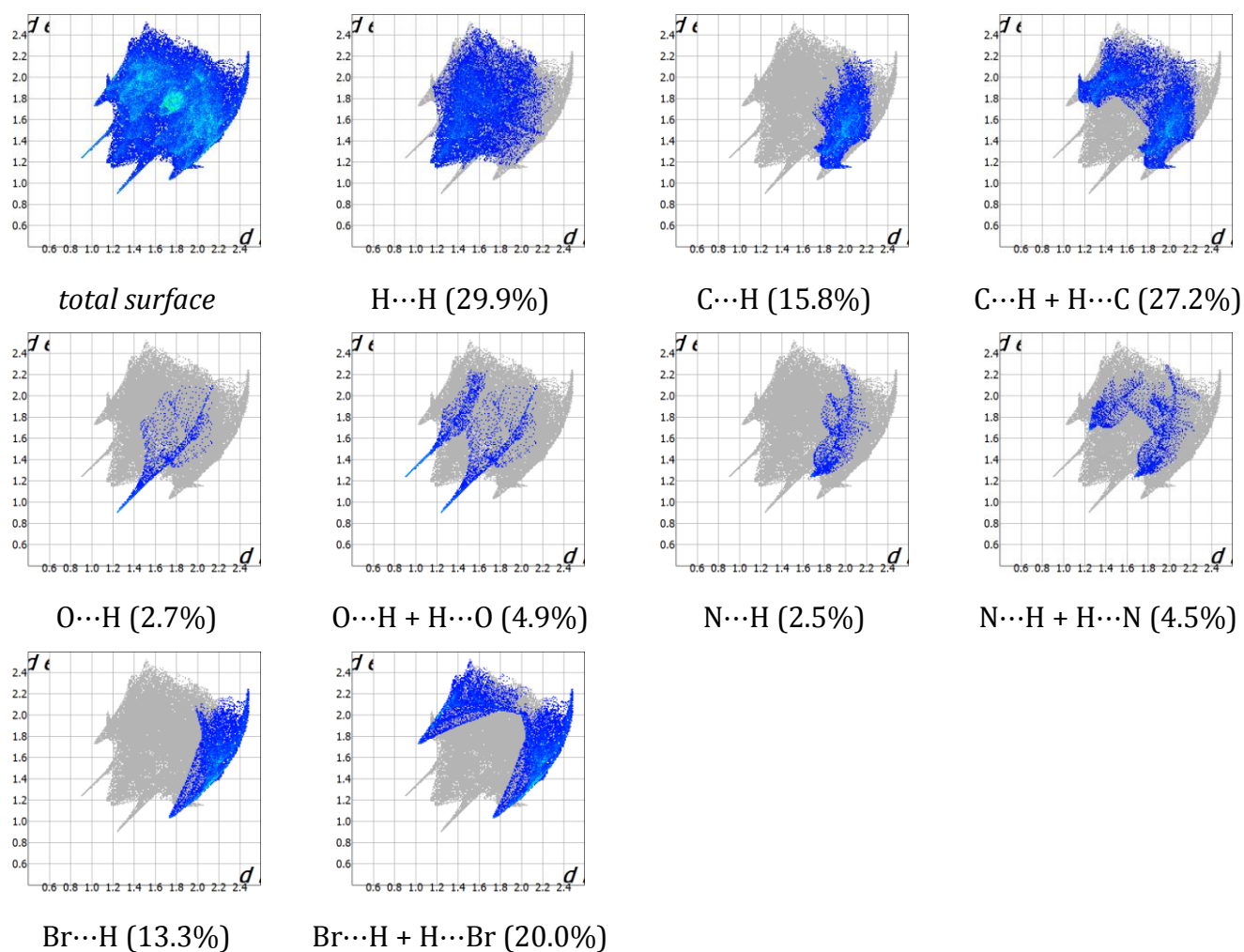


Figure 5S. Hirshfeld surface fingerprint plots for compound **c** showing various interactions contributions to the total surface (in X...Y the X atom is always inside and Y outside the surface).

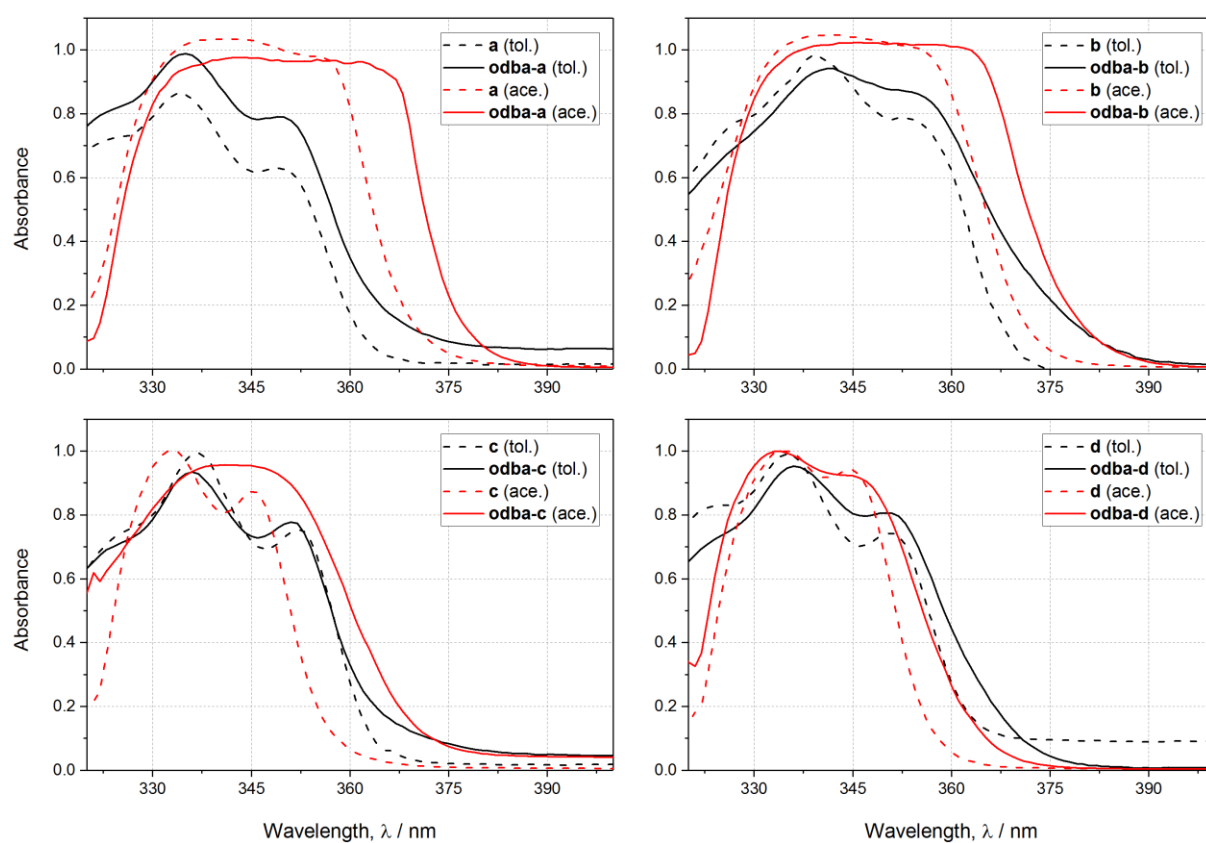


Figure 6S. UV-Vis absorption spectra for the (N,O)-donor compounds and their **odba** complexes measured in both toluene (tol.) and acetone (ace.).

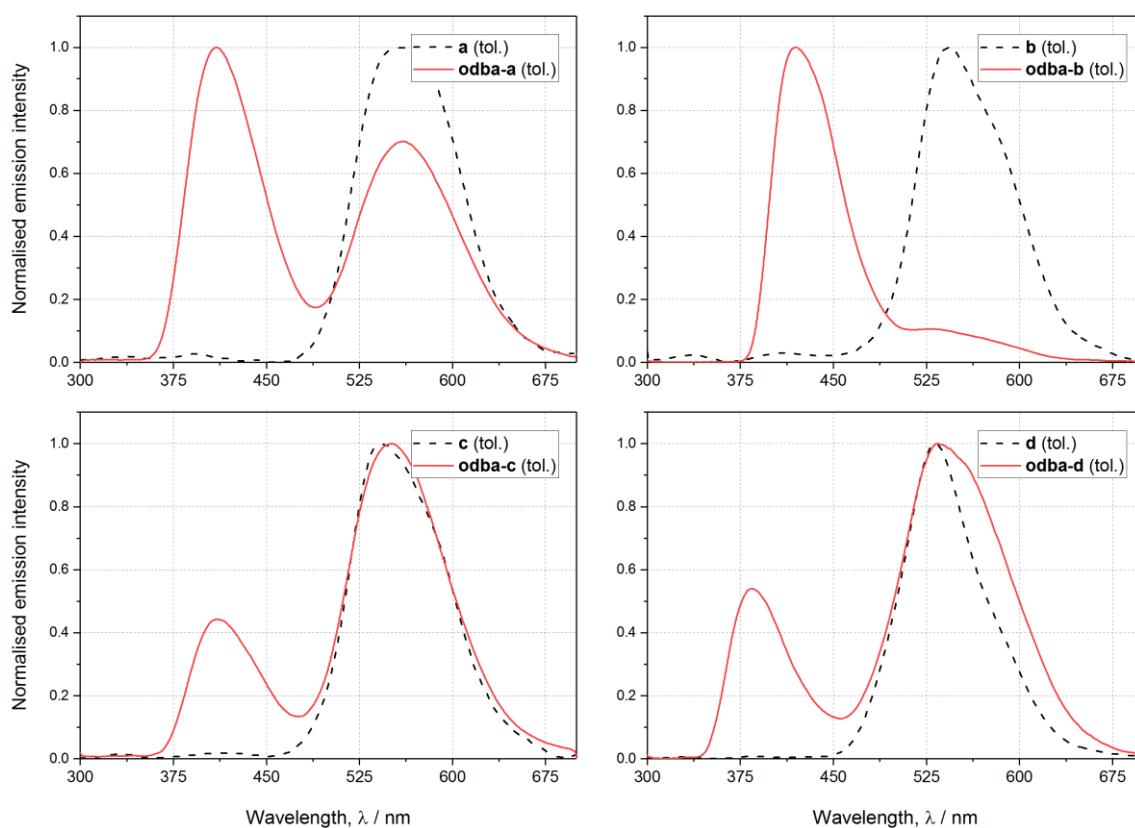


Figure 7S. Emission spectra for studied the (N,O)-donor compounds and their **odba** complexes measured in both toluene (tol.) (excitation wavelength, $\lambda_{\text{ex}} = 330$ nm).

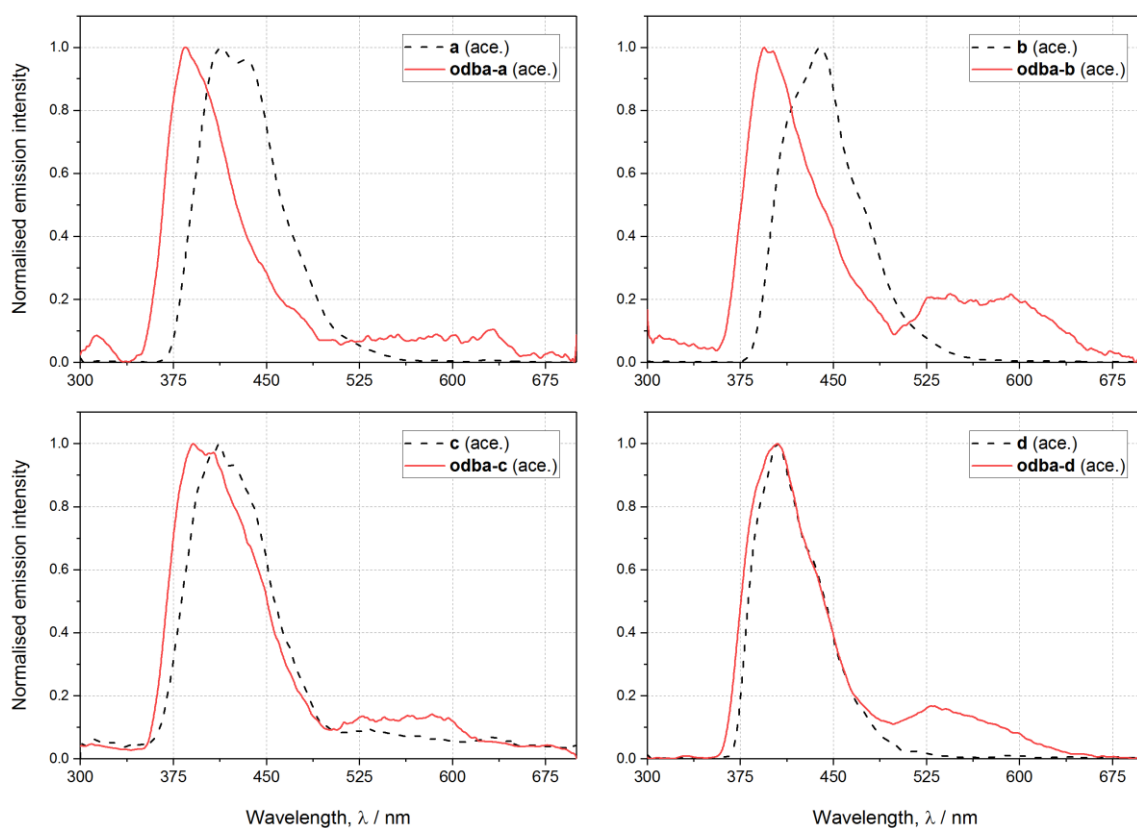


Figure 8S. Emission spectra for studied the (N,O)-donor compounds and their **odba** complexes measured in both acetone (ace.) (excitation wavelength, λ_{ex} = 315 nm for **a**, **odba-a**, **b**, **odba-b**, **c** & **odba-c**, and λ_{ex} = 330 nm for **d** & **odba-d**).

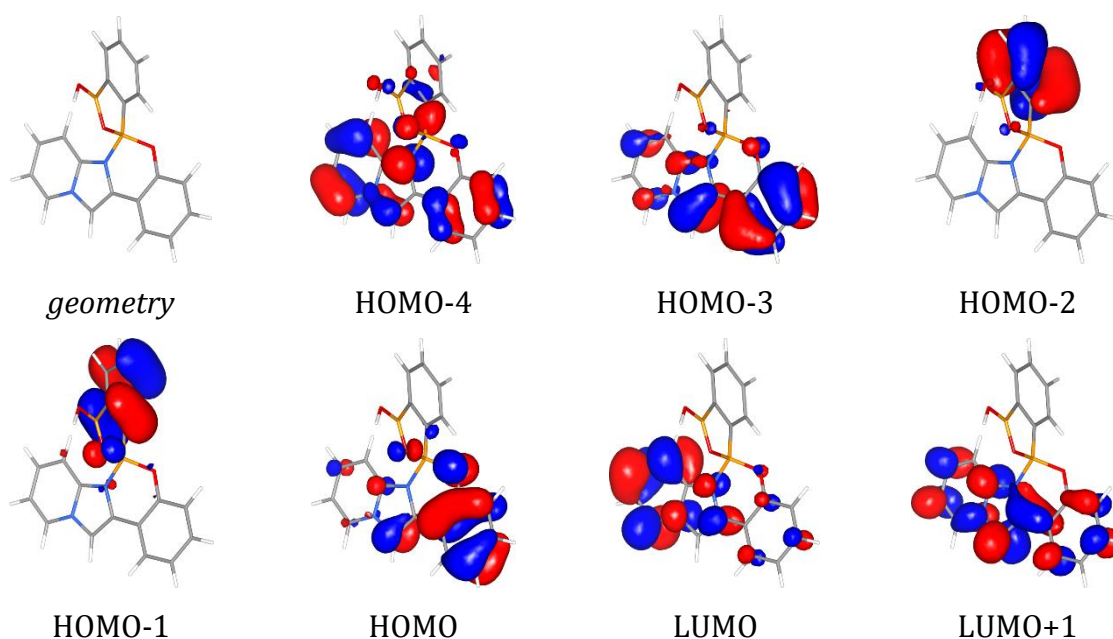


Figure 9S. Selected molecular orbitals for the **odba-a** molecule calculated at the DFT(B3LYP)/6-311++G** level of theory (geometry optimised at the same level; isosurfaces drawn at 0.035 a.u, blue – positive, red – negative).

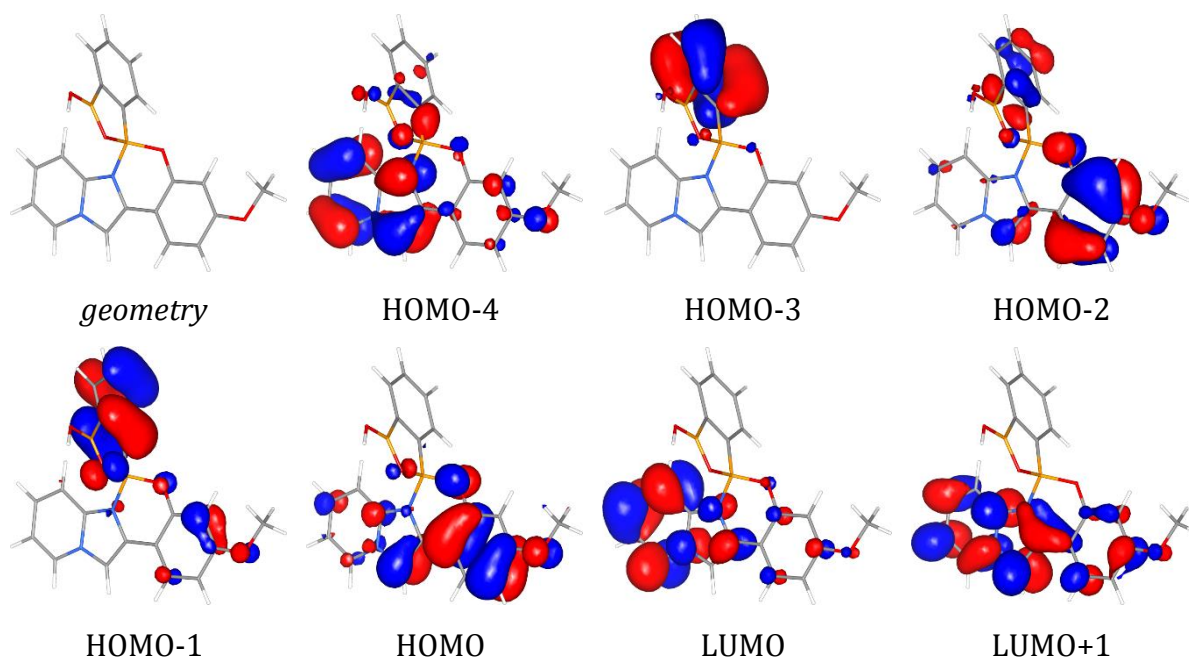


Figure 10S. Selected molecular orbitals for the **odba-b** molecule calculated at the DFT(B3LYP)/6-311++G** level of theory (geometry optimised at the same level; isosurfaces drawn at 0.035 a.u, blue – positive, red – negative).

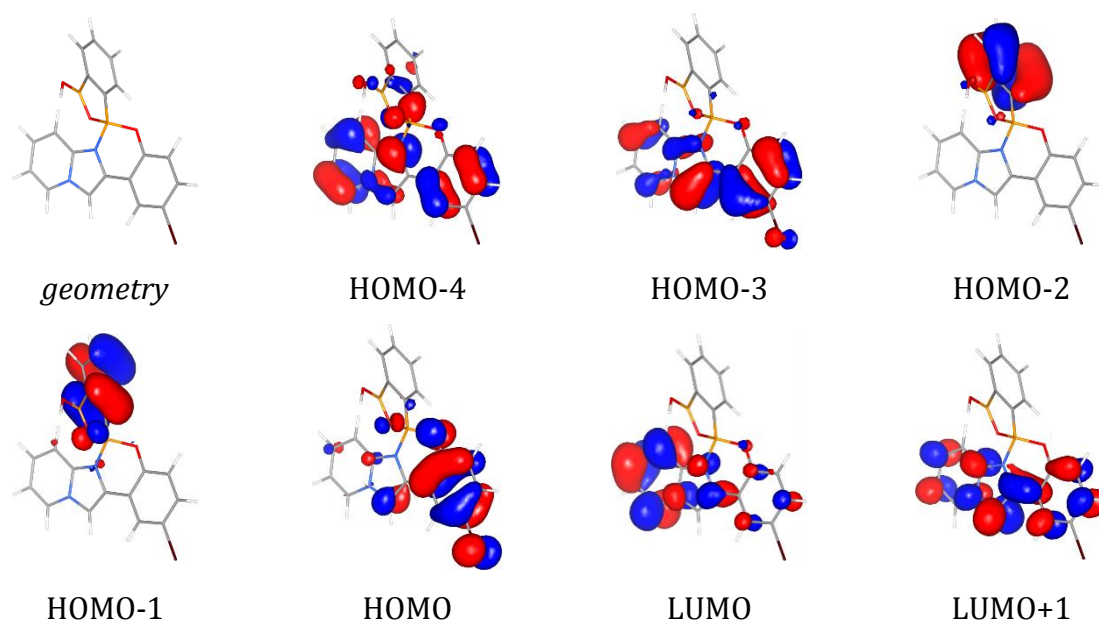


Figure 11S. Selected molecular orbitals for the **odba-c** molecule calculated at the DFT(B3LYP)/6-311++G** level of theory (geometry optimised at the same level; isosurfaces drawn at 0.035 a.u, blue – positive, red – negative).

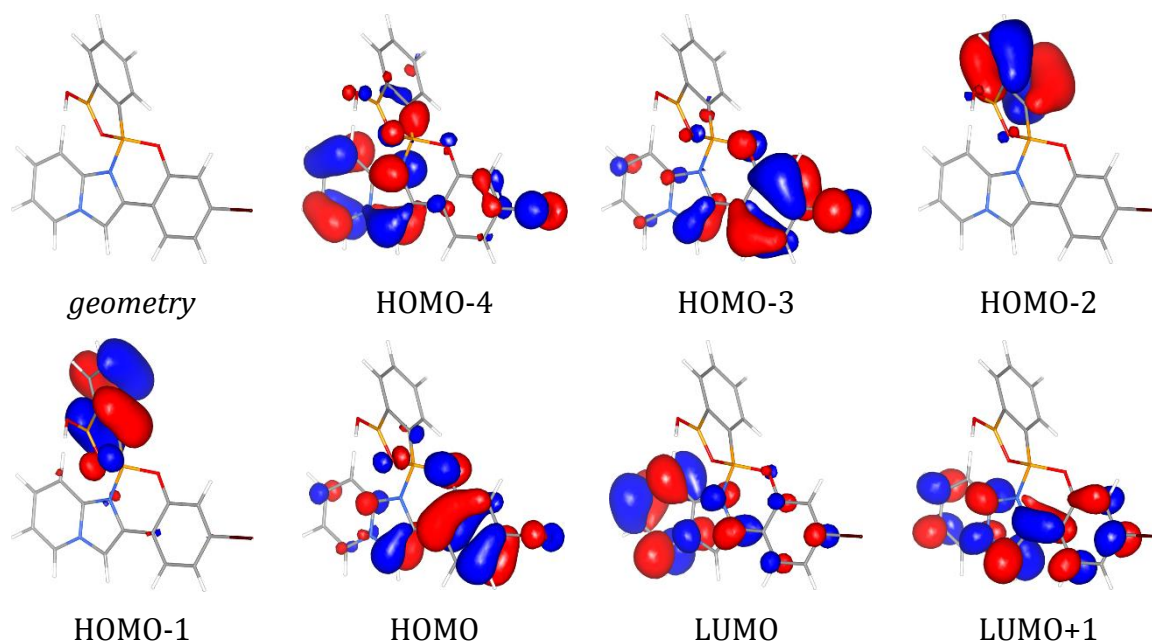


Figure 12S. Selected molecular orbitals for the **odba-d** molecule calculated at the DFT(B3LYP)/6-311++G** level of theory (geometry optimised at the same level; isosurfaces drawn at 0.035 a.u, blue – positive, red – negative).

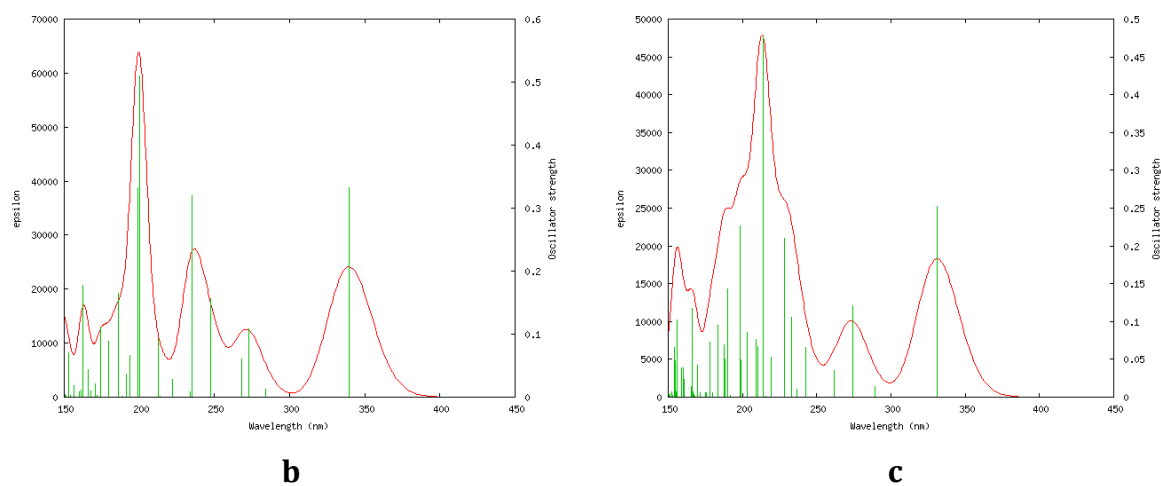


Figure 13S. TDDFT-evaluated UV-Vis spectra (DFT(PBE0)/6-31G** level of theory) for compounds **b** and **c** (crystal structure geometries). Oscillator strengths are marked as green bars; red-line envelope was drawn using default *GAUSSSUM* program settings.

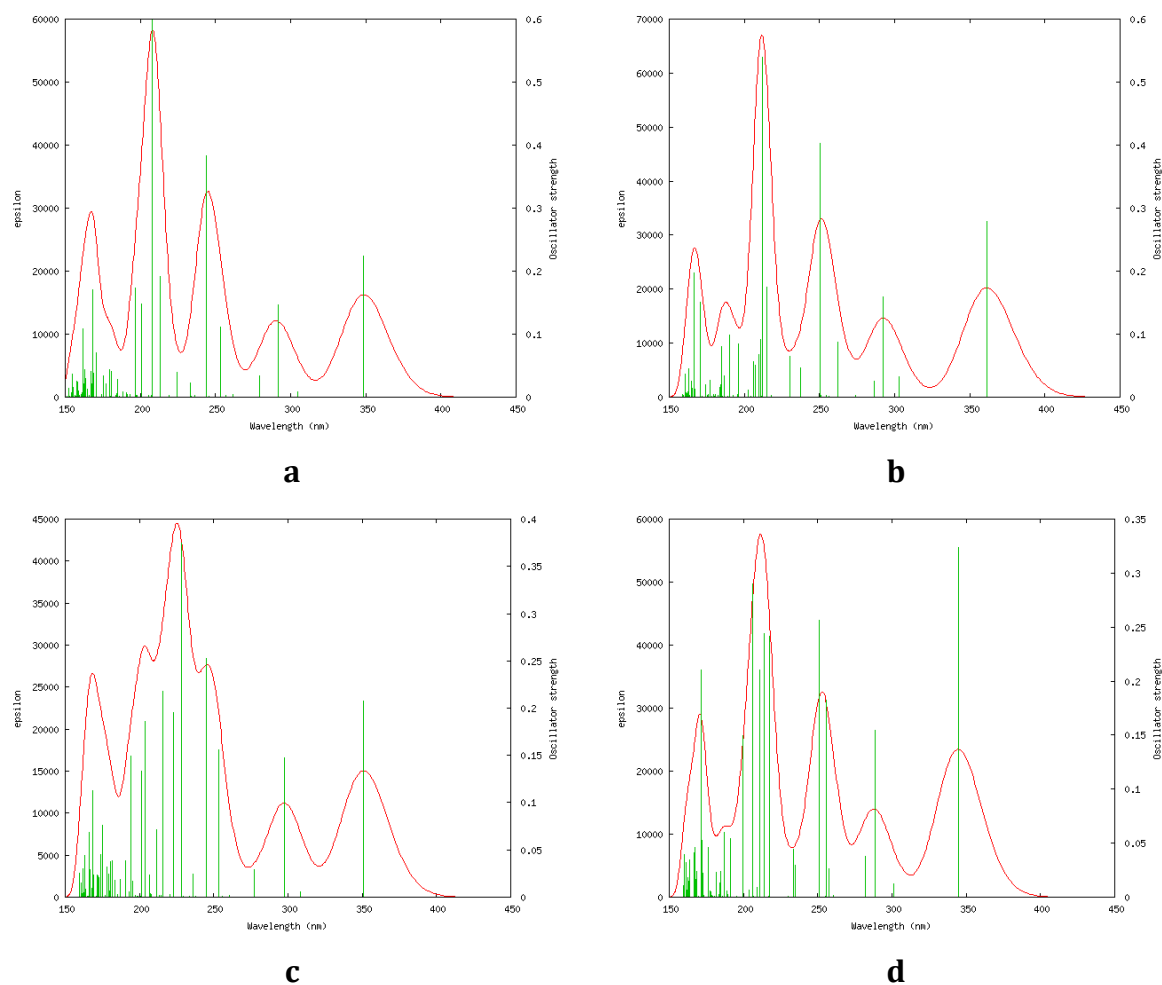


Figure 14S. TDDFT-evaluated UV-Vis spectra (DFT(B3LYP)/6-311++G** level of theory) for compounds **a** – **d** (optimised geometries). Oscillator strengths are marked as green bars; red-line envelope was drawn using default *GAUSSSUM* program settings.

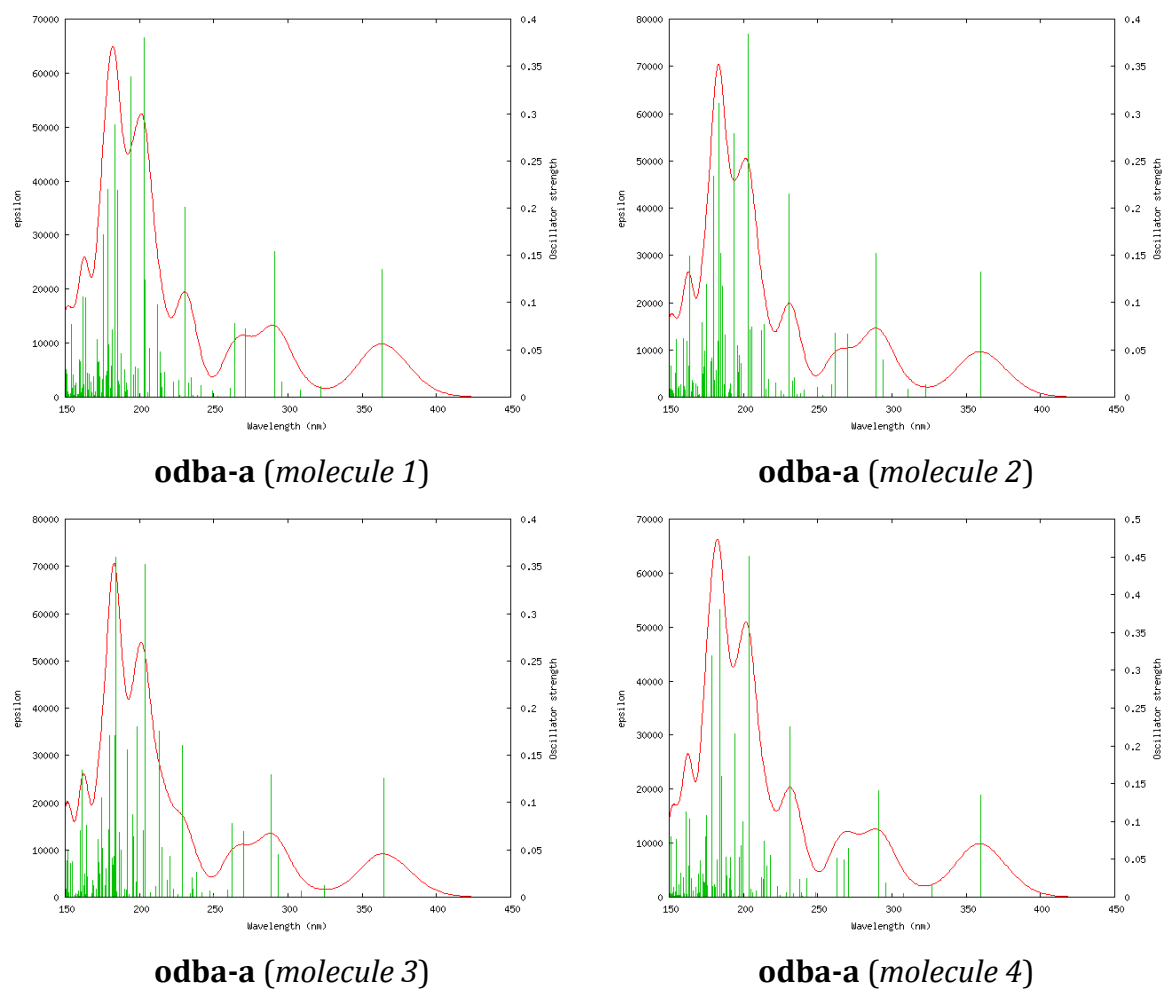


Figure 15S. TDDFT-evaluated UV-Vis spectra (DFT(PBE0)/6-31G** level of theory) for compound **odba-a** (crystal structure geometries). Oscillator strengths are marked as green bars; red-line envelope was drawn using default *GAUSSSUM* program settings.

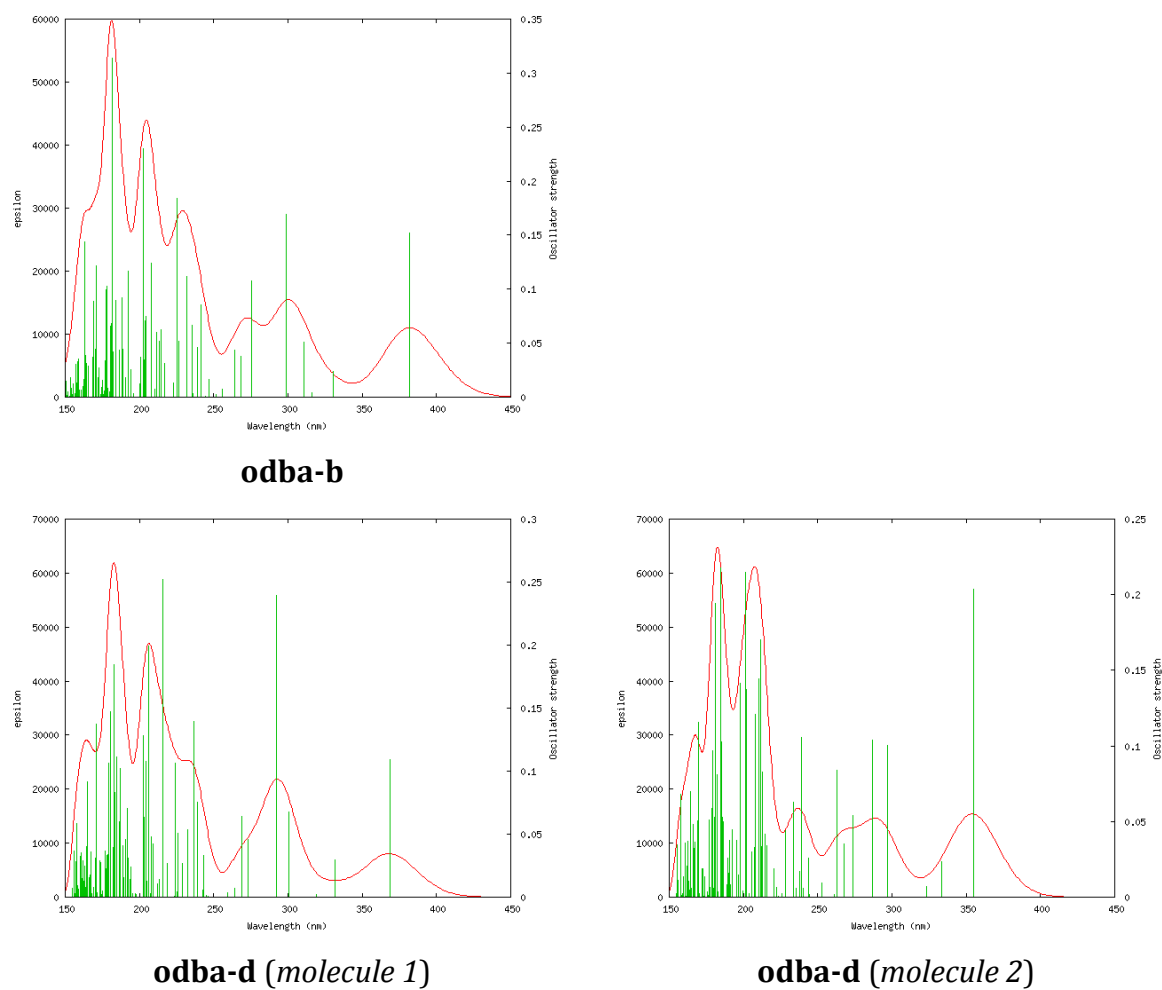


Figure 16S. TDDFT-evaluated UV-Vis spectra (DFT(PBE0)/6-31G** level of theory) for compounds **odba-b** and **odba-d** (crystal structure geometries). Oscillator strengths are marked as green bars; red-line envelope was drawn using default *GAUSSSUM* program settings.

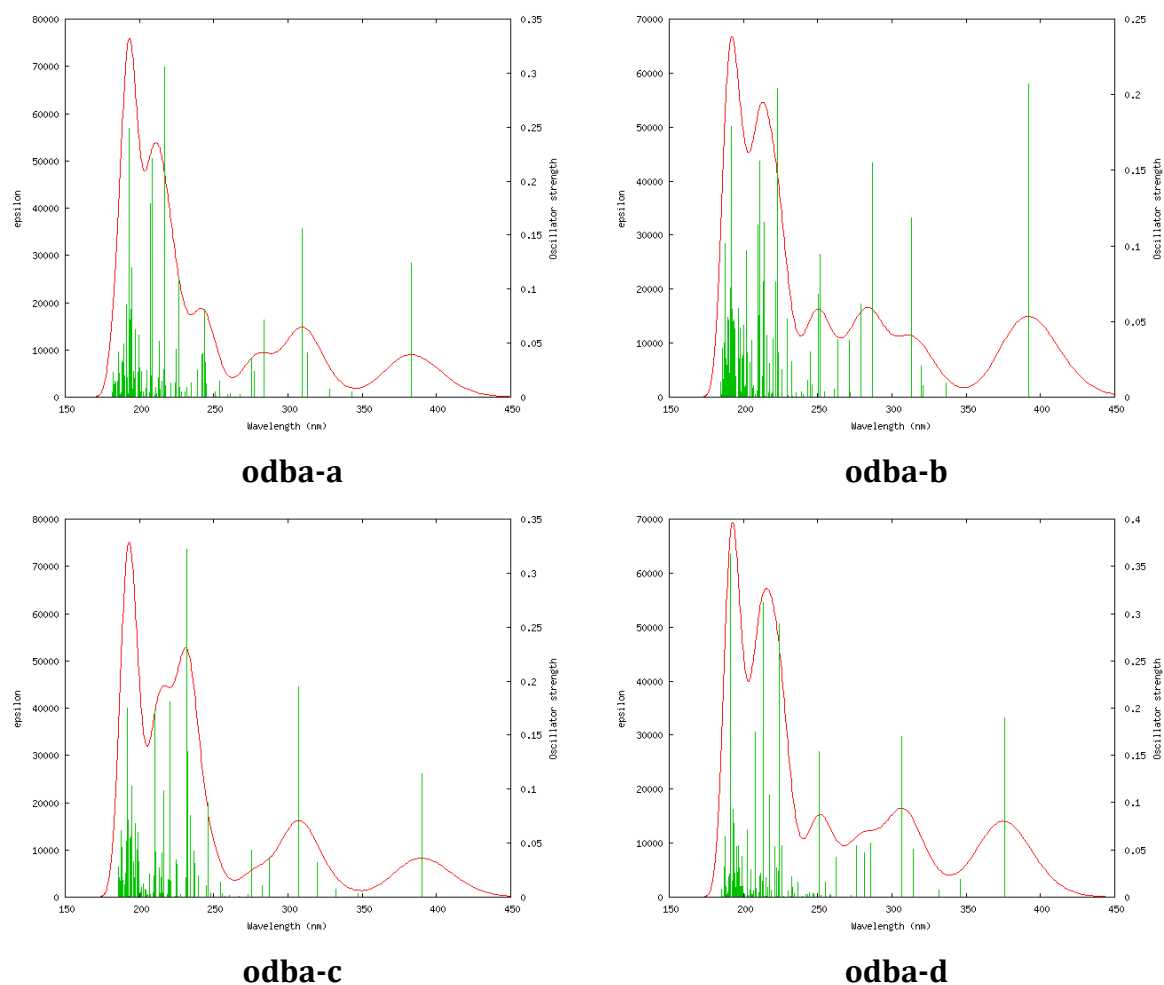


Figure 17S. TDDFT-evaluated UV-Vis spectra (DFT(B3LYP)/6-311++G** level of theory) for compounds **odba-a**, **odba-b**, **odba-c** and **odba-d** (optimised geometries). Oscillator strengths are marked as green bars; red-line envelope was drawn using default *GAUSSSUM* program settings.

Table 2S. Electrostatic-potential fitted charges computed at the DFT(B3LYP)/6-311++G** level of theory for all studied ligand derivatives together with other similar complexes (abbreviations: *p*-Cl = chlorine atom in *para* position to the OH group in the 6-membered aromatic ring *etc.*). All structures were optimised at the same level of theory.

Compound	Atom						
	O1	N1	N2	C1	C6	C7	C8
a	-0.648	-0.650	+0.448	+0.405	-0.637	+0.424	-0.193
<i>p</i> -Me	-0.655	-0.671	+0.456	+0.386	-0.665	+0.517	-0.252
<i>m</i> -Me	-0.648	-0.660	+0.469	+0.377	-0.681	+0.513	-0.312
<i>p</i> -OMe	-0.646	-0.709	+0.282	+0.527	-0.578	+0.500	-0.187
b = <i>m</i> -OMe	-0.634	-0.648	+0.511	+0.335	-0.731	+0.564	-0.390
<i>p</i> -F	-0.646	-0.671	+0.442	+0.392	-0.655	+0.513	-0.226
<i>m</i> -F	-0.628	-0.658	+0.462	+0.381	-0.673	+0.507	-0.317
<i>p</i> -Cl	-0.649	-0.666	+0.452	+0.395	-0.677	+0.515	-0.331
<i>m</i> -Cl	-0.621	-0.646	+0.451	+0.393	-0.646	+0.442	-0.170
c = <i>p</i> -Br	-0.647	-0.650	+0.471	+0.389	-0.685	+0.487	-0.347
d = <i>m</i> -Br	-0.629	-0.650	+0.448	+0.406	-0.639	+0.419	-0.138

Table 3S. TDDFT-calculated five lowest energy singlet-singlet transitions at the DFT(B3LYP)/6-311++G** level of theory (E – energy, f – oscillator strength; major transition contributions are shown in bold).

<i>Compound</i>	<i>E / eV</i>	<i>λ / nm</i>	<i>f · 10⁴</i>	<i>Main orbital contributions</i>
odba-a	3.24	383	1238	HOMO → LUMO
	3.61	343	49	HOMO-1 → LUMO
	3.78	328	77	HOMO-2 → LUMO
				HOMO-4 → LUMO+1
	3.96	313	411	HOMO-3 → LUMO HOMO → LUMO+1
	4.00	309	1562	HOMO-3 → LUMO HOMO → LUMO+1
<i>Compound</i>	<i>E / eV</i>	<i>λ / nm</i>	<i>f · 10⁴</i>	<i>Main orbital contributions</i>
odba-b	3.16	392	2096	HOMO → LUMO
				HOMO-2 → LUMO
	3.68	337	95	HOMO-1 → LUMO
	3.87	321	79	HOMO-3 → LUMO
				HOMO-2 → LUMO
	3.88	320	206	HOMO-1 → LUMO HOMO → LUMO+1
	3.96	313	1183	HOMO-2 → LUMO HOMO → LUMO+1
<i>Compound</i>	<i>E / eV</i>	<i>λ / nm</i>	<i>f · 10⁴</i>	<i>Main orbital contributions</i>
odba-c	3.18	390	1141	HOMO → LUMO
	3.57	347	30	HOMO-1 → LUMO
	3.73	332	71	HOMO-2 → LUMO
	3.87	320	324	HOMO-3 → LUMO HOMO → LUMO+1
				HOMO-4 → LUMO+1
	4.04	307	1948	HOMO-3 → LUMO HOMO → LUMO+1
<i>Compound</i>	<i>E / eV</i>	<i>λ / nm</i>	<i>f · 10⁴</i>	<i>Main orbital contributions</i>
odba-d	3.30	376	1901	HOMO → LUMO
	3.58	346	184	HOMO-1 → LUMO
	3.74	332	79	HOMO-2 → LUMO

3.95	314	505	HOMO-3 → LUMO HOMO → LUMO+1
4.04	307	1696	HOMO-3 → LUMO HOMO → LUMO+1